Calculated Magnetization Curves and Hybrid-Order Phase Transition of the d=1 Ising Model with Long-Range Power-Law Interactions

E. Can Artun[1, 2] and A. Nihat Berker[3, 2, 4]

[1] *TUBITAK Research Institute for Fundamental Sciences (TBAE), Gebze, Kocaeli 41470, Turkey*
[2] *Faculty of Engineering and Natural Sciences, Kadir Has University, Cibali, Istanbul 34083, Turkey*
[3] *Faculty of Engineering, MEF University, Maslak, Istanbul 34396, Turkey*
[4] *Department of Physics, Massachusetts Institute of Technology, Cambridge, Massachusetts 02139, USA*

The $d = 1$ Ising ferromagnet and spin glass with long-range power-law interactions $J\,r^{-a}$ are studied for all interaction range exponents a by a renormalization-group transformation that simultaneously projects local ferromagnetism and antiferromagnetism. In the ferromagnetic case, $J > 0$, a finite-temperature ferromagnetic phase occurs for interaction range $0.74 < a < 2$. The second-order phase transition temperature monotonically decreases between these two limits. At $a = 2$, the phase transition becomes first order, also as predicted by rigorous results. For $a > 2$, the phase transition temperature discontinuously drops to zero and for $a > 2$ there is no ordered phase above zero temperature, also as predicted by rigorous results. At the other end, on approaching $a = 0.74$ from above, namely increasing the range of the interaction, the phase transition temperature diverges to infinity, meaning that, at all non-infinite temperatures, the system is ferromagnetically ordered. Thus, the equivalent-neighbor interactions regime is entered before ($a > 0$) the neighbors become equivalent, namely before the interactions become equal for all separations. The critical exponents $\alpha, \beta, \gamma, \delta, \eta, \nu$ are calculated, from a large recursion matrix, varying as a function of a. For the antiferromagnetic case, $J < 0$, all triplets of spins at all ranges have competing interactions and this highly frustrated system does not have an ordered phase. In the spin-glass system, where all couplings for all separations are randomly ferromagnetic or antiferromagnetic (with probability p), a finite-temperature spin-glass phase is obtained, in the absence of antiferromagnetic phase. A truly unusual phase diagram is obtained. In the spin-glass phase, the signature chaotic behavior under scale change occurs in a richer version than previously: In the long-range interaction of this system, the interactions at every separation become chaotic, yielding a piecewise chaotic interaction function.

I. ORDERING IN ONE DIMENSION: LONG-RANGE INTERACTIONS

Whereas systems with finite-range interactions do not order above zero temperature in one dimension, certain systems with long-range interactions do order.[1–5] The archetypical example are the Ising ferromagnetic models with power-law interactions, $J\,r^{-a}$. Also as seen below, for antiferromagnetic interactions, the system incorporates saturated frustration and spin-glass ordering without antiferromagnetic ordering, in the absence of quenched randomness.

The model that we study is defined by the Hamiltonian

$$-\beta\mathcal{H} = \sum_{r_1 \neq r_2} J\,|r_1 - r_2|^{-a} s_{r_1} s_{r_2} + H \sum_{r_1} s_{r_1} \qquad (1)$$

where $\beta = 1/k_B T$ is the inverse temperature, r_1 and r_2 designate the sites on the one-dimensional system, at each site r_i there is an Ising spin $s_{r_i} = \pm 1$, and the sums are over all sites in the system. For ferromagnetic and antiferromagnetic systems, the two-spin interactions J are $J = |J| > 0$ and $J = -|J| < 0$, respectively. For the spin-glass system, for each two spins at any range, their interaction is randomly ferromagnetic (with probability $1 - p$) or antiferromagnetic (with probability p). The second term in Eq. (1) is the magnetic-field H term.

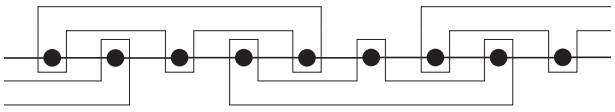

FIG. 1. Renormalization-group cells for $d = 1$. This cell structure projects both local ferromagnetism and antiferromagnetism, and therefore can also project spin-glass order.

II. METHOD: LONG-RANGE RENORMALIZATION GROUP

We solve this system with Niemeyer and van Leeuwen's two-cell cluster approximation.[6–8] The renormalization-group transformation is constructed by first choosing cells on the $d = 1$ system, as shown in Fig. 1. Each of our cells has three spins. This cell structure projects both local ferromagnetism and antiferromagnetism, and therefore can also project spin-glass order. Secondly, for each cell, a cell-spin is defined as the sign of the sum of the three spins in the cell,

$$s'_{r'} = signum(s_{r-2} + s_r + s_{r+2}) \qquad (2)$$

where the signum function returns the sign of its argument, primes denote the renormalized system, and $r' = r/b$, where $b = 3$ is the length-rescaling factor of the renormalization-group transformation. The renor-

malized interactions are obtained from the conservation of the partition function Z,

$$Z = \sum_{\{s\}} e^{-\beta\mathcal{H}(\{s\})} = \sum_{\{s'\}}\sum_{\{\sigma\}} e^{-\beta\mathcal{H}(\{s'\},\{\sigma\})} = \sum_{\{s'\}} e^{-\beta\mathcal{H}'(\{s'\})} = Z' , \quad (3)$$

where the summed variable σ represents, for each cell, the four states that give the same cell-spin value. Thus, the renormalized interactions are obtained from

$$e^{-\beta\mathcal{H}'(\{s'\})} = \sum_{\{\sigma\}} e^{-\beta\mathcal{H}(\{s'\},\{\sigma\})} . \quad (4)$$

The two-cell cluster approximation of Niemeyer and van Leeuwen consists in carrying out this transformation for two cells, including the 6 intracell interactions and the 9 intercell interactions. A recursion relation is obtained for each renormalized interaction,

$$J'_{r'} = \frac{1}{4}\ln\frac{R_{r'}(+1,+1)R_{r'}(-1,-1)}{R_{r'}(+1,-1)R_{r'}(-1,+1)} ,$$
$$H' = \frac{1}{4}\ln\frac{R_1(+1,+1)}{R_1(-1,-1)} , \quad (5)$$

where

$$R_{r'}(s'_0, s'_{r'}) = \sum_{\sigma_0,\sigma_{r'}} e^{-\beta\mathcal{H}_{0r'}} , \quad (6)$$

where the unrenormalized two-cell Hamiltonian contains the six intracell interactions and the 9 intercell interactions between the 6 spins in cells 0 and r'.

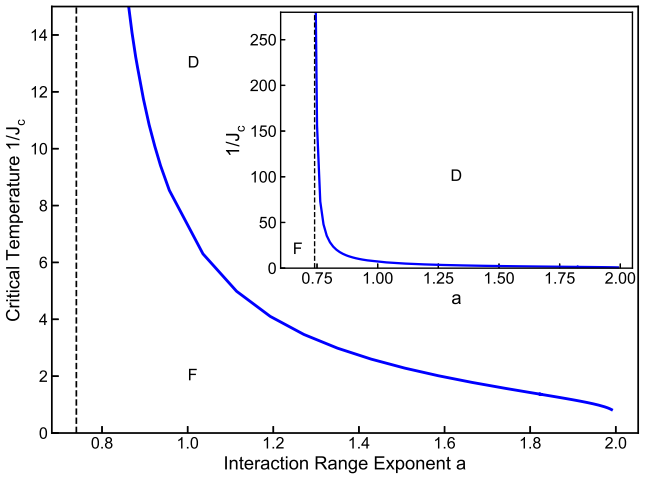

FIG. 2. Calculated phase diagram of the $d = 1$ long-range ferromagnetic Ising model with interactions $J\,r^{-a}$. Ferromagnetic (F) and disordered (D) phases are seen. A finite-temperature ferromagnetic phase transition occurs for $0.74 < a < 2$. The second-order phase transition temperature monotonically decreases between these two limits. At $a = 2$, the transition becomes first-order, as predicted by rigorous results [5] and also as seen from our calculated magnetization curves in Fig. 6 below. For $a > 2$ the phase transition temperature discontinuously drops to zero and there is no ordered phase above zero temperature, also as predicted by rigorous results [2, 3]. At the other end, towards the equivalent-neighbor limit, on approaching $a = 0.74$ from above, the phase transition temperature diverges to infinity, meaning that, at all non-infinite temperatures, the system is ferromagnetically ordered. Thus, the equivalent-neighbor interactions regime is entered before ($a > 0$) the neighbors become equivalent, namely before the interactions become equal for all separations. To the left of the dashed line on this figure is the equivalent-neighbor regime.

III. FINITE-TEMPERATURE FERROMAGNETIC PHASE TRANSITION IN $d = 1$ BETWEEN SHORT-RANGE AND EQUIVALENT-NEIGHBOR CUTOFFS

The calculated phase diagram of the $d = 1$ long-range ferromagnetic Ising model, with interactions $J\,r^{-a}$, is shown in Fig. 2, in terms of temperature $1/J$ and interaction range a. A finite-temperature second-order ferromagnetic phase transition occurs for $0.74 < a < 2$, which as seen below respectively are the equivalent-neighbor cutoff and the short-range cutoff. The second-order phase transition temperature monotonically decreases between these two limits. At $a = 2$, the phase transition becomes first order, as predicted by rigorous results [5] and also as seen from our calculated magnetization curves shown below. For $a > 2$ the phase transition temperature discontinuously drops to zero and there is no ordered phase above zero temperature, also as predicted by rigorous results [2, 3]. At the other end, namely with the longest-range including infinite-range interactions, on approaching $a = 0.74$ from above, the phase transition temperature diverges to infinity, meaning that, at all non-infinite temperatures, the system is ferromagnetically ordered. The interactions renormalize to infinity for all non-zero starting values. Thus, the equivalent-neighbor interactions regime is entered in fact before ($a > 0$) the neighbors become equivalent, namely before the interactions become equal for all separations. Rigorous results [2, 3] show that a strong coupling regime is entered at exactly $a = 1$. Thus, our calculated value is an approximation to $a = 1$, whereas at the lesser long-range end of the ordering, the exact $a = 2$ is rendered by our calculation.

The calculated correlation-length critical exponent ν, correlation-function critical exponent η, specific heat critical exponent α, magnetization critical exponents β and δ, susceptibility critical exponent γ, continuously varying as a function of interaction range exponent a for the finite-temperature ferromagnetic phase transition, are shown in Fig. 3. These critical exponents are calculated, with $H = H' = 0$, from the recursion relations $J'_1, ..., J'_n = \text{funct}(J_1, ..., J_n)$ of Eqs. (5,6). Convergence

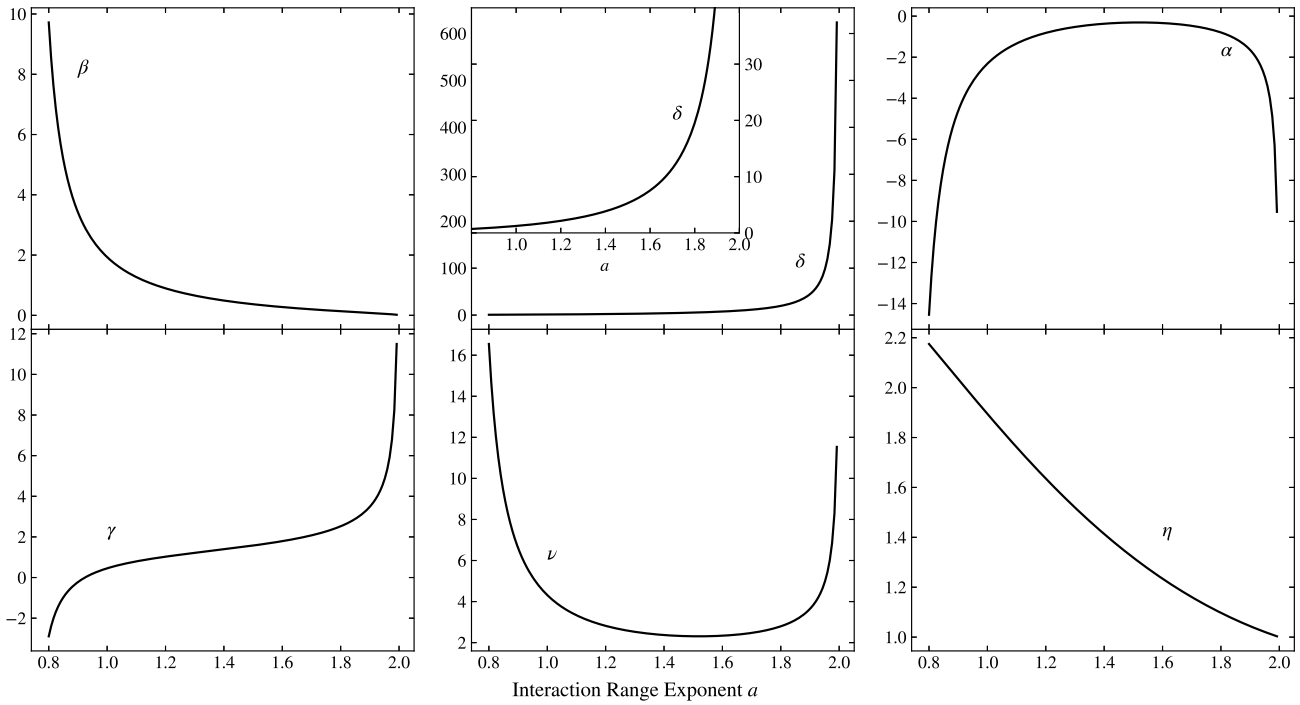

FIG. 3. Correlation-length critical exponent ν, correlation-function critical exponent η, specific heat critical exponent α, magnetization critical exponents β and δ, susceptibility critical exponent γ, as a function of interaction range a for the finite-temperature ferromagnetic phase transition. Note that β reaches 0 and δ, γ diverge to infinity, as expected, as the first-order phase transition as $a = 2$ is reached from below. However, at $a = 2$, ν and α respectively reach plus and minus infinity, giving an unobservable essential singularity of the specific heat. Thus the phase transition at $a = 2$ is hybrid order.

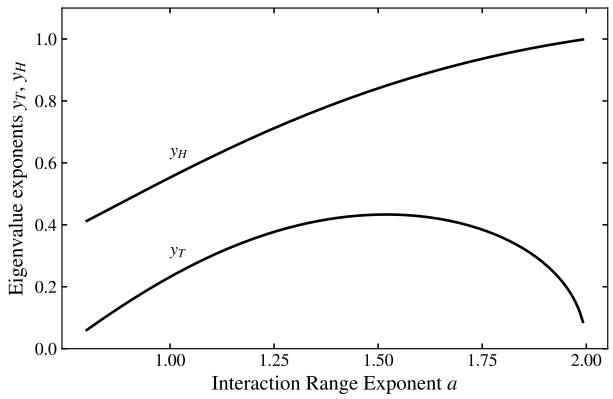

FIG. 4. Calculated thermal and magnetic eigenvalue exponents y_T and y_H, as a function of the interaction range exponent a. These y_T and y_H respectively go to 0 and $d = 1$ as $a = 2$ is approached, respectively giving an essential singularity for the thermal thermodynamic functions and a discontinuity for the magnetization, in all meaning a hybrid-order phase transition.

is obtained by calculation up to $n = 20$. The largest (and, as expected, only relevant, namely greater than 1) eigenvalue $\lambda_T = b^{y_T}$ of the derivative matrix (so-called recursion matrix) $\mathbf{T} = \partial J'_k/\partial J_l$ of these recursion relations at the fixed point $\mathbf{J}^*_\mathbf{n}$ of the recursion relations gives the correlation-length critical exponent $\nu = 1/y_T$ and the specific heat critical exponent $\alpha = 2 - d/y_T = 2 - 1/y_T$. For each a, the 20-dimensional renormalization-group flow about the (convergedly calculated for $n = 20$ below) fixed point $\mathbf{J}^*_\mathbf{n}$ of the phase transiton is unstable, but is nevertheless found precisely from the Newton-Raphson procedure,

$$\mathbf{J}^* = (\mathbf{T} - \mathbf{I})^{-1}(\mathbf{T} \cdot \mathbf{J} - \mathbf{J}'), \tag{7}$$

which is a matrix-vector product equation, where prime refers to the renormalized interaction, $\mathbf{I}$ is the identity matrix, and the recursion matrix $\mathbf{T}$ is calculated at $\mathbf{J}$. A few iterations of this procedure gives $\mathbf{J}^*$ precisely. Fig. 4 shows the calculated fixed-point interactions J^*_n as a function of the interaction range exponent a. The eigenvalue exponents y_T and y_H are shown in Fig. 5 and respectively go to 0 and 1 as $a = 2$ is approached from below, as expected for the exponents explained below.

The magnetization critical exponents $\beta = (d - y_H)/y_T = (1 - y_H)/y_T$ and $\delta = y_H/(d - y_H) = y_H/(1 - y_H)$, the susceptibility critical exponent $\gamma = (2y_H - d)/y_T$, and the correlation-function critical exponent $\eta = 2 + d - y_H = 3 - y_H$ are calculated, at the critical fixed point $\mathbf{J}^*$, with $H = H' = 0$, from

$\partial H'/\partial H = b^{y_H}$.[8] Note that at $a = 2$, the magnetization critical exponent $\beta = 0$, which is required for a first-order phase transition [9] as temperature is scanned. At $a = 2$, the other magnetization critical exponent δ and the susceptibility critical exponent γ diverge to infitinity, which gives the first-order transition as the magnetic field is scanned. At $a = 2$, the correlation length critical exponent ν diverges to plus infinity and the specific heat critical exponent diverges to minus infinity (thus having an invisible essential singularity [10]), as in the $d = 2$ XY model transition [11, 12]. However, unlike the $d = 2$ XY model, the low-temperature phase has a calculated non-zero magnetization, saturating at zero temperature and going discontinuously to zero at the finite-temperature phase transition (Fig. 5), making the phase transition at $a = 2$ a hybrid-order phase transition [13].

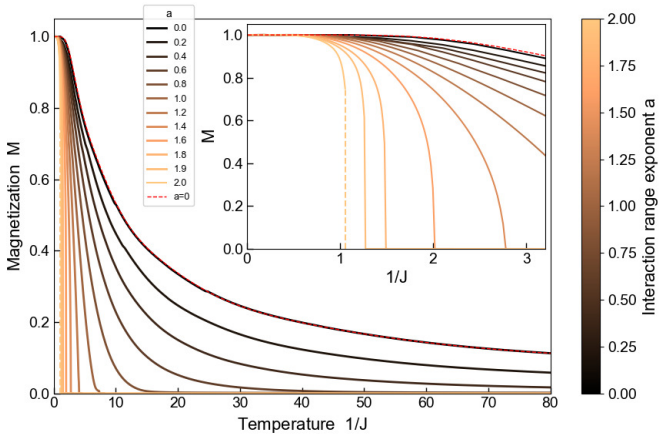

FIG. 5. Calculated magnetization curves for different values of the interaction range critical exponent a. For the less-long-range threshold of $a = 2$, the dashed line shows the discontinuity in the magnetization. For $a < 0.74$, the magnetization decays with temperature but remains non-zero.

IV. CALCULATED MAGNETIZATION CURVES: HYBRID-ORDER PHASE TRANSITION

Magnetization curves $M(T)$ are calculated by multiplying, along the renormalization-group trajectory, the magnetization recursion relation,

$$M_0 = b^{-n} M_n \cdot \left(\frac{\partial H'}{\partial H}\right)_n \cdots \left(\frac{\partial H'}{\partial H}\right)_2 \cdot \left(\frac{\partial H'}{\partial H}\right)_1, \qquad (8)$$

where the subscript n designates the nth renormalization-group transformation along the trajectory. Even when starting close to the phase transition, the trajectory takes this product close to a phase-sink fixed point. At the disordered phase sink, $M_n = 0$, and thus at the trajectory starting temperature $M_0 = 0$. At the ferromagnetic ordered phase sink, $M_n = 1$ and $(\partial H'/\partial H)_n = b$, and thus at the starting non-zero magnetization is calculated.

The thus calculated magnetization curves for the entire range of temperatures for each a are given in Fig. 6. For $0.74 < a < 2$, the magnetization curves show a second-order phase transition, with the magnetizations continuously reaching zero as the critical temperature is approached from below. The second-order phase transition temperature monotonically decreases between these two limits of a. At $a = 2$, the phase transition becomes first order, as seen by the large discontinuity in calculated magnetization only at $a = 2$. For $a > 2$ the phase transition temperature discontinuously drops to zero and there is no ordered phase above zero temperature, also as predicted by rigorous results [2, 3]. At the other end, on approaching $a = a_{eq} = 0.74$ from above, the phase transition temperature diverges to infinity. For $a < a_{eq}$, the calculated magnetization is non-zero at all non-infinite temperatures as seen Fig. 6, and the system is ferromagnetically ordered. Thus, the equivalent-neighbor interactions regime is entered in fact before ($a > 0$) the neighbors become equivalent, namely before the interactions become equal for all separations. To the left of the dashed line on this figure is the equivalent-neighbor regime.

V. FINITE-TEMPERATURE SPIN-GLASS PHASE IN $d = 1$ WITHOUT ANTIFERROMAGNETIC PHASE

The antiferromagnetic, overly frustrated without randomness, system does not have a finite-temperature phase transition, as all renormalization-group trajectories flow to the disordered phase sink fixed pont. However, the spin-glass system, where all couplings for all separations are randomly ferromagnetic or antiferromagnetic (with probability p), does have finite-temperature spin-glass phase transitions and chaos inside the spin-glass phase, as seen in Fig. 7. This truly unusual spin-glass phase diagram, actually does not have an antiferromagnetic phase but has a spin-glass phase. Nevertheless, typical spin-glass system reentrance [15] is seen in this phase diagram, where as temperature is lowered at fixed antiferromagnetic bond concentration p, the ferromagnetic phase appears, but disappears at further lower temperature.

The spin-glass phase shows its signature of chaos under rescaling [16–19], but in a richer version than previously: In the long-range interaction of this system, the interactions at every separation become chaotic, as seen in the lower panel of Fig. 7, yielding an interaction potential that is piecewise chaotic.

For a previous $d = 1$ Ising spin-glass study, with short-range interactions and a zero-temperature spin-glass phase, see [20].

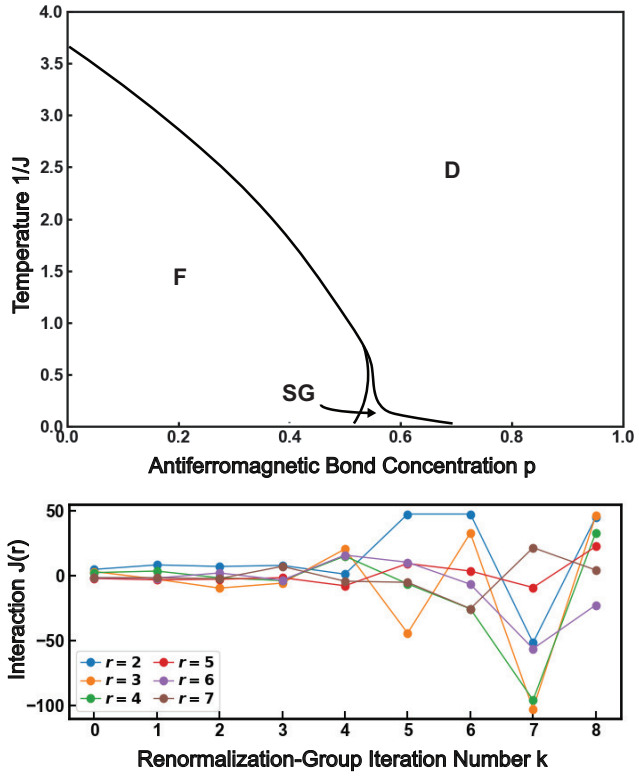

FIG. 6. Calculated finite-temperature phase diagram of the $d = 1$ long-range Ising spin-glass system with interaction-range exponent $a = 1$, where all couplings for all separations are randomly ferromagnetic or antiferromagnetic (with probability p). Ferromagnetic (F), spin-glass (SG), and disordered (D) phases are seen. This truly unusual spin-glass phase diagram, actually does not have an antiferromagnetic phase but has a spin-glass phase. Bottom panel: Chaos inside the spin-glass phase in $d = 1$. The spin-glass phase shows the chaos under rescaling signature [16–19], in a richer version than previously: In the long-range interaction of this system, the interactions at every separation become chaotic, as seen in the lower panel of this figure, yielding a piecewise chaotic interaction potential.

VI. CONCLUSION

We have solved the $d = 1$ Ising ferromagnet, antiferromagnet, and spin glass with long-range power-law interactions $J\,r^{-a}$, for all interaction range exponents a by a renormalization-group transformation that simultaneously projects local ferromagnetism, antiferromagnetism, and spin-glass order. In the ferromagnetic case, $J > 0$, a finite-temperature second-order ferromagnetic phase occurs for interaction range $0.74 < a < 2$. The second-order phase transition temperature monotonically decreases between these two limits. The critical exponents $\alpha, \beta, \gamma, \delta, \eta, \nu$ for the second-order phase transitions are calculated, from a large recursion matrix, varying as a function of a. At $a = 2$, the phase transition becomes first order, as predicted by rigorous results. For $a > 2$, the phase transition temperature discontinuously drops to zero and for $a > 2$ there is no ordered phase above zero temperature, also as predicted by rigorous results. At the other end, towards the equivalent-neighbor limit, on approaching $a = 0.74$ from above, namely increasing the range of the interaction, the phase transition temperature diverges to infinity, meaning that, at all non-infinite temperatures, the system is ferromagnetically ordered. Thus, the equivalent-neighbor interactions regime is entered before ($a > 0$) the neighbors become equivalent, namely before the interactions become equal ($a = 0$) for all separations.

For the antiferromagnetic case, $J < 0$, all triplets of spins at all ranges have competing interactions and this highly frustrated system does not have an ordered phase.

In the spin-glass system, where all couplings for all separations are randomly ferromagnetic or antiferromagnetic (with probability p), a finite-temperatures spin-glass phase is obtained, in the absence of antiferromagnetic phase. A truly unusual phase diagram, with reentrance around the ferromagnetic phase, is obtained. In the spin-glass phase, the signature chaotic behavior under scale change occurs in a richer version than previously: In the long-range interaction of this system, the interactions at every separation become chaotic, yielding a piecewise chaotic interaction function.

ACKNOWLEDGMENTS

Support by the Academy of Sciences of Turkey (TÜBA) is gratefully acknowledged.

[1] D. J. Thouless, Long-Range Order in One-Dimensional Ising Systems, Phys. Rev. **187**, 732 (1969).
[2] D. Ruelle, Statistical Mechanics Rigorous Results (Benjamin, New York, 1969).
[3] R. B. Griffiths, Rigorous Results and Theorems, in Phase Transitions and Critical Phenomena, edited by C. Domb and M. S. Green (Academic, New York, 1972), Vol. 1.
[4] M. Aizenman and C. Newman, Discontinuity of the Percolation Density in One-Dimensional $1/[X - Y]^2$ Percolation Models, Comm. Math. Phys. **107**, 611 (1986).
[5] M. Aizenman, J. Chase, L. Chase, and C. Newman, Discontunuity of the Magnetization in One-Dimensional $1/|x - y|^2$ Ising and Potts Models, J. Stat. Phys. **50**, 1 (1988).

[6] T. Niemeyer and J. M. J. van Leeuwen, Physica (Utr.) **71**, 17 (1974).

[7] J. M. J. van Leeuwen, Singularities in the Critical Surface and Universality for Ising-Like Spin Systems, Phys. Rev. Lett. **34**, 1056 (1975).

[8] A. N. Berker and M. Wortis, Blume-Emery-Griffiths-Potts Model in Two Dimensions: Phase Diagram and Critical Properties from a Position-Space Renormalization Group, Phys. Rev. B **14**, 4946 (1976).

[9] M. E. Fisher and A. N. Berker, Scaling for First-Order Phase Transitions in Thermodynamic and Finite Systems Phys. Rev. B **26** 2507 (1982).

[10] A. N. Berker and D. R. Nelson, Superfluidity and phase separation in helium films, Phys. Rev. B **19**, 2488 (1979).

[11] J. M. Kosterlitz and D. J. Thouless, Ordering, metastability and phase transitions in two-dimensional systems, J. Phys. C **6**, 1181 (1973).

[12] J. V. José, L. P. Kadanoff, S. Kirkpatrick, and D. R. Nelson, Renormalization, vortices, and symmetry-breaking perturbations in two-dimensional planar model, Phys. Rev. B **16**, 1217 (1977).

[13] S. R. McKay and A. N. Berker, Equimagnetization Lines in the Hybrid-Order Phase Diagram of the d=3 Random-Field Ising Model, J. Appl. Phys. **4**, 5785 (1988).

[14] E. C. Artun and A. N. Berker, Complete Density Calculations of q-State Potts and Clock Models: Reentrance of Interface Densities under Symmetry Breaking, Phys. Rev. E **102**, 062135 (2020).

[15] M. Hinczewski and A. N. Berker, Multicritical Point Relations in Three Dual Pairs of Hierarchical-Lattice Ising Spin Glasses, Phys. Rev. E **72**, 144402 (2005).

[16] S. R. McKay, A. N. Berker, and S. Kirkpatrick, Spin-glass behavior in frustrated Ising models with chaotic renormalization-group trajectories, Phys. Rev. Lett. **48**, 767 (1982).

[17] S. R. McKay, A. N. Berker, and S. Kirkpatrick, Amorphously packed, frustrated hierarchical models: Chaotic rescaling and spin-glass behavior, J. Appl. Phys. **53**, 7974 (1982).

[18] S. R. McKay and A. N. Berker, J. Appl. Phys., Chaotic Spin Glasses: An Upper Critical Dimension, J. Appl. Phys. **55**, 1646 (1984).

[19] A. N. Berker and S. R. McKay, Hierarchical Models and Chaotic Spin Glasses, J. Stat. Phys. **36**, 787 (1984).

[20] G. Grinstein, A. N. Berker, J. Chalupa, and M. Wortis, Phys. Exact Renormalization Group with Griffiths Singularities and Spin-Glass Behavior: The Random Ising Chain, Phys. Rev. Lett. **50**, 1 (1988).